Kinetics of liquid-mediated crystallization of amorphous Ge from multi-frame dynamic TEM

M.K. Santala[1,a,b], S. Raoux[2,c], G.H. Campbell[1]

[1]Materials Science Division, Lawrence Livermore National Laboratory, 7000 East Ave., Livermore, CA 94551, USA

[2]Helmholtz-Zentrum Berlin für Materialien und Energie GmbH, Hahn-Meitner-Platz 1, D-14109, Berlin, Germany

The kinetics of laser-induced, liquid-mediated crystallization of amorphous Ge thin films were studied using multi-frame dynamic transmission electron microscopy (DTEM), a nanosecond-scale photo-emission transmission electron microscopy technique. In these experiments, high temperature gradients are established in thin amorphous Ge films with a 12-ns laser pulse with a Gaussian spatial profile. The hottest region at the center of the laser spot crystallizes in ~100 ns and becomes nano-crystalline. Over the next several hundred nanoseconds crystallization continues radially outward from the nano-crystalline region forming elongated grains, some many microns long. The growth rate during the formation of these radial grains is measured with time-resolved imaging experiments. Crystal growth rates exceed 10 m/s, which is consistent with crystallization mediated by a very thin, undercooled transient liquid layer, rather than a purely solid-state transformation mechanism. The kinetics of this growth mode have been studied in detail under steady-state conditions, but here we provide a detailed study of liquid-mediated growth in high temperature gradients. Unexpectedly, the propagation rate of the crystallization front was observed to remain

---

[a] Author to whom correspondence should be addressed. Electronic mail: melissa.santala@oregonstate.edu

[b] Current address: Mechanical, Industrial, and Manufacturing Engineering, Oregon State University, 204 Rogers Hall, Corvallis, OR 97331

[c] Current address: Helmholtz-Zentrum Berlin für Materialien und Energie GmbH, Hahn-Meitner-Platz 1, D-14109, Berlin, Germany

constant during this growth mode even when passing through large local temperature gradients, in stark contrast to other similar studies that suggested the growth rate changed dramatically. The high throughput of multi-frame DTEM provides gives a more complete picture of the role of temperature and temperature gradient on laser crystallization than previous DTEM experiments.

Laser crystallization of amorphous semiconductor thin films is an important processing path for electronic devices. It is possible to achieve a variety of grain sizes and textures with laser processing, including very large grain sizes, which are useful for thin-film solar cells,[1] metal-oxide-semiconductor field-effect transistors, and thin film transistors.[2] Laser processing can also create metastable and unstable transient states that are inaccessible with other processing methods resulting in distinctive microstructures that are of scientific and practical interest. When heating an amorphous semiconductor slowly, crystallization begins hundreds of degrees below the equilibrium crystalline melting temperature, T_m, in a solid-state transformation.[3,4] With the extremely high heating rates accessible with laser heating, it is possible to locally form a non-equilibrium liquid phase below T_m, before crystallization occurs.

It was hypothesized in 1979 that a first order transition, distinct from a glass transition, exists between the semiconducting amorphous state and the metallic liquid state of Ge and Si and that the transition occurs at a temperature well below T_m.[5,6] Based on available thermodynamic data, the amorphous-liquid transition temperature, T_{ma}, for Ge was estimated to be ~969 K,[5] well below Ge's T_m of 1210 K. The stated implication of this hypothesis was that the presence of a highly undercooled liquid may result in high nucleation rates and extremely fast crystal growth,[5] both of which have be observed during laser crystallization.[7,8-13]

The microstructure resulting from laser crystallization of amorphous Ge varies with the characteristics of the laser pulse and the thermal properties of the thin film and substrate. Figure 1(a) shows a transmission electron microscope (TEM) image of a laser-crystallized region of 50-nm amorphous Ge film supported on a 20-nm amorphous silicon nitride membrane. The Ge was deposited by magnetron sputtering at room temperature (T_{RT}) and was amorphous as deposited. The laser-crystallized area was produced by exposure of the film to a 532-nm laser pulse of 3.4 μJ and 12-ns full-width half-maximum (FWHM) duration. It has many of microstructural features observed by others[8-10,14,15] during pulse laser-crystallization of amorphous semiconductors in a thin electron transparent geometry. The central region, which we call Zone I, is nanocrystalline (grain diameter < 100 nm) as a result of extremely high nucleation rates achieved in the hottest part of the specimen. Zone I is surrounded by large grains - some many microns long - that have their major axes directed radially (Zone II), parallel to direction of crystal growth. Zone II is surrounded by long grains that spiral around the crystallized region and have their major axes oriented tangentially to the preceding crystallized material (Zone III). The large grains in Zone III are interleaved with fine-grained, feathery-appearing crystalline material.

This study focuses on Zone II growth, where the nucleation rate is low and extremely rapid, liquid-mediated growth occurs. Previous time-resolved TEM studies on pulse laser crystallization have measured growth rates of ~8 - 12 m/s in Zone II.[9,10,15] Since completely solid state crystallization would be orders of magnitude slower,[3,16] the rapid crystal growth is reasoned to be mediated by a thin layer of undercooled liquid formed ahead of the crystalline front by the heat released during crystallization.[9,10] Experimental observations, including dopant re-distribution,[17] surface texture changes,[17,18] and reflectance[19,20] and conductance changes,[11,12,19,21] provide additional evidence for the existence of a liquid layer during the

extremely rapid crystal growth in amorphous semiconductors that is sometimes called "explosive" crystallization.[22] During explosive crystallization, a liquid layer, just a few nanometers thick,[20,23] forms ahead of the crystalline front by the heat of crystallization released during the phase transformation. The energy released raises the adjacent amorphous material above the T_{ma}, but the liquid is undercooled and crystallizes very rapidly. The liquid layer is continually re-generated at the crystallization front, provided heat losses to the environment are not too great. In TEM specimens initially at T_{RT}, heat loss from laser-heated areas is low because the specimen is only tens of nanometers thick, but crystallization quenches as the front propagates from the laser-heated region into cooler parts of the thin film.

By maintaining the Ge substrate temperature, T_s, well above T_{RT}, steady-state explosive crystallization may be maintained across an entire specimen.[11-13] The role of T_s and heat loss on crystallization rate was studied by two groups[11,12,13] using Ge films on thick substrates maintained at a fixed temperature. Both groups found explosive crystallization propagated without quenching if the substrate was >600K (higher for thinner films). Propagation rates started at ~1 m/s and increased with increasing temperature, until they saturated at ~700K. Chojnacka[12] found the growth rate saturated at ~13 m/s for 1.3 − 3 μm thick films for T_s from ~670 K (for thick films) to ~820 K. Grigoropoulos *et al.*[13] found growth rates saturated at ~9 m/s for T_s from 700 to 800 K with 0.89 and 1.8-μm Ge films. At lower T_s (~600-700 K), heat loss from the Ge to the substrate is high, the growth rate was very sensitive to changes in temperature, and the resulting microstructure was "scalloped" with the growth direction of large grains parallel to the growth front, like Zone III growth in laser-crystallized TEM specimens. At high T_s (~700-800 K), heat loss to the substrate is low, the growth rate was temperature insensitive, and columnar grains grew perpendicular to the growth front, similar to the growth

mode in Zone II.[9,10] The microstructural similarities occur because Zone II develops near the hot center of the laser spot and the transition to Zone III (scalloped microstructure) occurs as growth propagates to cooler regions of the specimen. Despite similarities between laser crystallization on electron transparent thin film and the steady-state experiments on heated bulk substrate, the TEM specimens initially at T_{RT} can have higher temperature gradients established by the Gaussian laser pulse (shown schematically in Figure 1(b,c)). Since our specimens start at T_{RT}, the crystallization quenches rapidly, but we are able to image the liquid-mediated explosive crystallization before quenching because of the high spatial and temporal resolution of the dynamic TEM (DTEM).

We studied Zone II crystallization kinetics in high temperature gradients using DTEM, a photo-emission TEM technique which allows us to resolve microstructural transformations on nanosecond-to-microsecond time scales. In DTEM, each high-current electron pulse contains enough electrons to form an image. DTEM has been used to study dynamic processes in a variety of materials,[24] including crystallization of amorphous Ge.[8-10] Previously, Ge was studied with "single-shot" DTEM, in which a single image is formed of each crystallization event. To study the process over time, single images of different reactions were accumulated to build an averaged view of the process over time. Zone II crystal growth rate for Ge was estimated at ~8 – 12 m/s in some single shot DTEM experiments[9] and to vary between 1 and 14 m/s,[10] a similar range of rates as measured during low heat loss, steady-state explosive crystallization.[11-13] In this work, multiple images are taken of each crystallization event. The DTEM at Lawrence Livermore National Laboratory, originally built as a single-shot DTEM, is now equipped with a laser system capable of generating multiple photo-emitted electron pulses spaced over nanoseconds or microseconds. An electrostatic deflector, installed below the instrument's

standard electron optics, deflects each image to a different part of the camera's charge-coupled device overcoming the camera's refresh rate. The design and operating principles of DTEM have been described in detail elsewhere.[25]

Crystallization experiments were performed in the DTEM on 50-nm amorphous Ge films deposited at T_{RT} using magnetron sputtering onto commercially-available TEM specimen supports with a 20-nm thick, 0.25×0.25 mm amorphous silicon nitride window and capped with 8 nm of silica. Sputtering was performed with 99.999% Ge target, using 25W dc power, and an Ar pressure of 2 mTorr; the deposition rate was 0.016 nm/s. Crystallization was induced with 3.3 to 4.9 µJ pulses from a frequency doubled Nd:YAG laser (532-nm wavelength, spatially Gaussian with 90 ± 5-µm $1/e^2$ diameter, temporally Gaussian 12-ns FWHM duration), directed onto the specimen ~42° from the specimen normal. Bright-field TEM images of each crystallization event were generated from nine 20-ns electron pulses with an interframe spacing of 95 ns. The delay between the specimen laser and the first electron image was varied from 25 to 800 ns to capture all of Zone II development. The extent of Zone II crystal growth at each time step was determined on low magnification (250X) images, *cf.* Figure 2(a), by fitting an ellipse to the crystalline Ge and taking half of the minor axis of the ellipse as the position of the front relative to the center of the laser spot. The final sizes of Zone I and II were similarly measured on conventional TEM images taken after laser crystallization. In higher magnification time-resolved images only small sections of the growth fronts are imaged and the position of the front of individual grains was tracked in each frame.

A typical set of DTEM images of Ge crystallization is shown in Figure 2(a). At 100-ns, a crystalline region in the center of the laser spot is already visible. Conventional TEM (Figure 1(a)) confirmed the central region consists of nanocrystalline grains, typical of Zone I growth.

Zone I consistently formed within 100 ns, similar to results from other experiments.[8] Zone II growth may proceed from crystalline material in Zone I without further nucleation events, however isolated nucleation occasionally occurs ahead of the main Zone II growth front, resulting in protrusions ahead of the elliptical front, as indicated by an arrow in Figure 2(a).

Crystallization was not observed for shot energies below 3.3 µJ. From 3.3 − 3.6 µJ, the Ge crystallized, but Zone I did not always form. Plotting Zone I size versus the laser shot energy (Figure 2(b)) shows a trend of Zone I increasing in size with increasing laser energy, though there is considerable spread in Zone I size at any laser energy; the sizes of Zones I, II, and III versus laser energy are provided in the Supplemental Material, Figure S1, at [26]. A systematic explanation for this variability in behavior for the same laser energy has not yet been found. The point lying at 0 µm is a crystallization event where Zone I did not form; growth instead proceeded outward in Zone II mode from one small site (Supplemental material, Figure S2, at [26]) that is microstructurally distinct from Zone I.

The Zone II growth front position imaged at 250X is plotted as a function of time in Figure 3(a). Uncertainty in position measurements arises from motion blur (which spreads the apparent interface by ~200 nm for a front advancing at ~10 m/s in a 20-ns exposure), low contrast between the crystalline and amorphous phases, and nucleation events ahead of the main Zone II front which distort the elliptical front shape making it difficult to determine position of the moving front to better than ±900 nm at 250X. The data for each crystallization event are relatively well fit by a line, indicating the growth front speed (the line's slope) is nearly constant during Zone II growth. Deviations from linearity in the data from laser energies above 4.3 µJ appear to be due to random scatter, rather than any consistent change of growth rate. For the two

data sets starting at 800 ns, growth rapidly stalls to ~1 m/s, because the transition to Zone III growth occurred, as verified with conventional TEM after crystallization.

Multi-frame DTEM experiments show unambiguously that Zone II growth propagates at high rates in the first hundred nanoseconds after Zone II formation and continues at a nearly constant rate until Zone III growth begins. This contrasts strikingly with growth rates reported from similar single-shot DTEM experiments by Nikolova *et al.*[10] where Zone II growth was said to start at ~1 m/s, accelerate to ~14 m/s, and then fall to ~2 m/s before the transition to Zone III growth. Those observations were based on single images from repeated crystallization experiments. Multi-frame DTEM images each crystallization event at multiple points in time, yielding a more accurate measure of the Zone II crystallization kinetics. Any ambiguity from the low resolution and relatively large error in low magnification DTEM movies is removed by higher magnification movies, which confirm the crystallization front can exceed 10 m/s within 100 ns of Zone II growth (Supplemental material, Figure S3, at [26]).

Zone II growth rates vary from 5.7 − 12.6 m/s but are nearly constant for each crystallization event. Initially it appears odd that Zone II growth is constant, since high temperature gradients are created by the laser pulse and crystallization is not occurring under steady state conditions, however, Grigoropoulos *et al.*[13] and Chojnacka[11,12] showed growth velocities may be constant rate for a range of T_s during steady-state explosive crystallization. Experiments and numerical heat flow calculations on Si by Stolk *et al.*[20] also showed growth may be constant for a range of temperatures near the maximum crystal interface speed for non-steady state experimental configuration. Molecular dynamics simulations by Albenze *et al.* of steady-state explosive crystallization in Ge and Si using a range of different temperature profiles suggested the crystallization rate depends most sensitively on the crystal-liquid interface temperature (with

little dependence on the liquid-amorphous interface temperature) and compensation for changes in heat-loss conditions occurs through self-rectification of the liquid layer width.[23] What is then striking in our results is that the rate may be constant over time for different growth rates. If the liquid-mediated Zone II growth rate were temperature insensitive for a range of temperatures as in Chojnacka's steady-state experiments, the growth rate might be expected to be self-adjusting over a range of temperatures and approach a single steady-state rate, but this is not the case. The challenge is to understand why there are different growth rates, but that each is constant, during Zone II growth through a rapidly changing temperature field.

Plotting the growth rate versus shot energy (Supplemental material, Figure S4, at [26]) yields no strong trend in the growth rate with laser energy, likely due to the variation in material response even for the same laser energy, *cf.* Figure 2(a). We normalize our data using the size of Zone I as a relative measure of laser energy absorption, and as an internal calibration point where we may estimate the temperature immediately after laser heating. The precipitous drop in nucleation rate between Zone I and II suggests existence of a temperature threshold at which there is a sharp change in atomic mobility, as may occur during amorphous melting. If amorphous melting indeed occurs inside the Zone I boundary upon laser heating, we expect the temperature at the Zone I/II boundary to have been initially near T_{ma}. Plotting growth rate against Zone I (Figure 3(b)) shows a stronger trend toward lower growths rates as the Zone I size increases. If we assume the initial temperature at the time of formation at the outer edge of Zone I is approximately the same for different shots, then different shots are differentiated not by the local temperature at the crystal growth front but by the local temperature gradient. Near the center of the laser spot the energy distribution is relatively flat and closer to the point of inflection of the Gaussian laser spot the temperature drops off more quickly. The gradient of the

9

energy distribution from the laser pulse with a $1/e^2$ radius of 45 μm increases in magnitude up to 22.5 μm radius. Thus, in our experiments Zone II growth rate decreases with increasing negative temperature gradient, or more rapid heat loss conditions. Since the heat loss is greater, Zone II growth should also quench and transition to Zone III more quickly, as seen in a plot of Zone I vs. Zone II size (Figure 3(c)).

These results show the growth rate may be influenced by the local temperature gradient upon initiation. Multi-frame DTEM provides a means to understand liquid-mediated crystallization of semi-conductors in the presence of high temperature gradients, though more work is required to clarify how the temperature, temperature gradient, and heat loss conditions impact the growth rate. We acknowledge there may be growth rate changes that we were not able to resolve, but multi-frame DTEM experiments show that Zone II growth rates do not fluctuate as widely as claimed in recent reports. The temperature at the crystal-liquid and liquid-amorphous interfaces are affected by heat absorbed (or evolved) by the phase transformations and by the re-distribution of the thermal energy from the laser pulse by heat flow through the specimen, but we do not have a means to experimentally measure the temperature at the interfaces. This has motivated a campaign of phase field modeling to clarify the connection between the spatio-temporal temperature profiles and the kinetics of crystal growth in these experiments. By systematically altering the temperature gradient by changing the base substrate temperature with a TEM cooling/heating holder and altering laser pulse shape, models may be tested against an expanded range of experimental conditions.

ACKNOWLEDGMENTS

REFERENCES

[1] J. Dore, D. Ong, S. Varlamov, R. Egan, and M.A. Green, IEEE Journal of Photovoltaics **4** (1), 33 (2014).

[2] N. H. Nickel, *Laser Crystallization of Silicon*. (Elsevier, London, 2003).

[3] P. Germain, K. Zellama, S. Squelard, J. C. Bourgoin, and A. Gheorghiu, J. Appl. Phys. **50** (11), 6986 (1979).

[4] H. Kanno, K. Toko, T. Sadoh, and M. Miyao, Appl. Phys. Lett. **89** (18), 182120 (2006); S. Yamaguchi, N. Sugii, S. K. Park, K. Nakagawa, and M. Miyao, J. Appl. Phys. **89** (4), 2091 (2001).

[5] B. G. Bagley and H. S. Chen, in *Laser-Solid Interactions and Laser Processing*, Materials Research Society, Boston, 1979.

[6] F. Spaepen and D. Turnbull, in *AIP Conference Proceedings*, Materials Research Society, Boston, 1979.

[7] R. L. Chapman, J. C. C. Fan, H. J. Zeiger, and R. P. Gale, Appl. Phys. Lett. **37** (3), 292 (1980); O. Bostanjoglo and G. Hoffmann, Phys. Status Solidi A-Appl. Res. **73** (1), 95 (1982); O. Bostanjoglo, W. Marine, and P. Thomsenschmidt, Appl. Surf. Sci. **54**, 302 (1992).

[8] L. Nikolova, T. LaGrange, B. W. Reed, M. J. Stern, N. D. Browning, G. H. Campbell, J. C. Kieffer, B. J. Siwick, and F. Rosei, Appl. Phys. Lett. **97** (20), 203102 (2010).

[9] L. Nikolova, T. LaGrange, M. J. Stern, J. M. MacLeod, B. W. Reed, H. Ibrahim, G. H. Campbell, F. Rosei, and B. J. Siwick, Phys. Rev. B **87** (6), 064105 (2013).

[10] L. Nikolova, M. J. Stern, J. M. MacLeod, B. W. Reed, H. Ibrahim, G. H. Campbell, F. Rosei, T. LaGrange, and B. J. Siwick, J. Appl. Phys. **116** (9), 093512 (2014).

[11] A. Chojnacka and M. O. Thompson, Growth, Evolution and Properties of Surfaces, Thin Films and Self-Organized Structures Symposium (Mater. Res. Soc. Proc.), 2001.

[12] A. P. Chojnacka, Ph.D. dissertation, Cornell University, 2002.

[13] C. Grigoropoulos, M. Rogers, S. H. Ko, A. A. Golovin, and B. J. Matkowsky, Phys. Rev. B **73** (18) (2006).

[14] O. Bostanjoglo, Phys. Status Solidi A-Appl. Res. **70** (2), 473 (1982); P. Pierrard, B. Mutaftschiev, W. Marine, J. Marfaing, and F. Salvan, Thin Solid Films **111** (2), 141 (1984); C. Cesari, G. Nihoul, J. Marfaing, W. Marine, and B. Mutaftschiev, Surface Science **162** (1-3), 724 (1985); O. Bostanjoglo and E. Endruschat, Phys. Status Solidi A-Appl. Res. **91** (1), 17 (1985).

[15] O. Bostanjoglo, R. P. Tornow, and W. Tornow, Ultramicroscopy **21** (4), 367 (1987).

[16] Ge growth data from 588 to 770 K [15], where only an amorphous-solid-to-crystal transition occurs, support the assertion that a transient liquid layer is needed for crystal growth on the order of 10 m/s. Extrapolating the data for the solid-solid transition, while taking the conservative position of ignoring the decreasing driving force for crystallization approaching Tm, still only yields a growth rate of ~100 µm/s at Tm, orders of magnitude below the actual Zone II crystal growth rates.

[17] H. J. Leamy, W. L. Brown, G. K. Celler, G. Foti, G. H. Gilmer, and J. C. C. Fan, Appl. Phys. Lett. **38** (3), 137 (1981).

[18] G. H. Gilmer and H. J. Leamy, in *Laser and Electron Beam Processing of Materials* Cambridge, MA, 1980.

[19] M. O. Thompson, G. J. Galvin, J. W. Mayer, P. S. Peercy, J. M. Poate, D. C. Jacobson, A. G. Cullis, and N. G. Chew, Physical Review Letters **52** (26), 2360 (1984).

[20] P. A. Stolk, A. Polman, and W. C. Sinke, Phys. Rev. B **47** (1), 5 (1993).

[21] M. O. Thompson, J. W. Mayer, A. G. Cullis, H. C. Webber, N. G. Chew, J. M. Poate, and D. C. Jacobson, Physical Review Letters **50** (12), 896 (1983).

[22] T. Takamori, R. Messier, and R. Roy, Appl. Phys. Lett., 201 (1972).

[23] E. J. Albenze, M. O. Thompson, and P. Clancy, Phys. Rev. B **70** (9) (2004).

[24] Geoffrey H. Campbell, Joseph T. McKeown, and Melissa K. Santala, Applied Physics Reviews **1** (4) (2014).

[25] T. LaGrange, B. W. Reed, M. K. Santala, J. T. McKeown, A. Kulovits, J. M. K. Wiezorek, L. Nikolova, F. Rosei, B. J. Siwick, and G. H. Campbell, Micron **43** (11), 1108 (2012);   T. Lagrange, B. Reed, and D. J. Masiel, MRS Bull. **40**, 22 (2015).

[26] See supplemental material at [*URL to be inserted by AIP*].
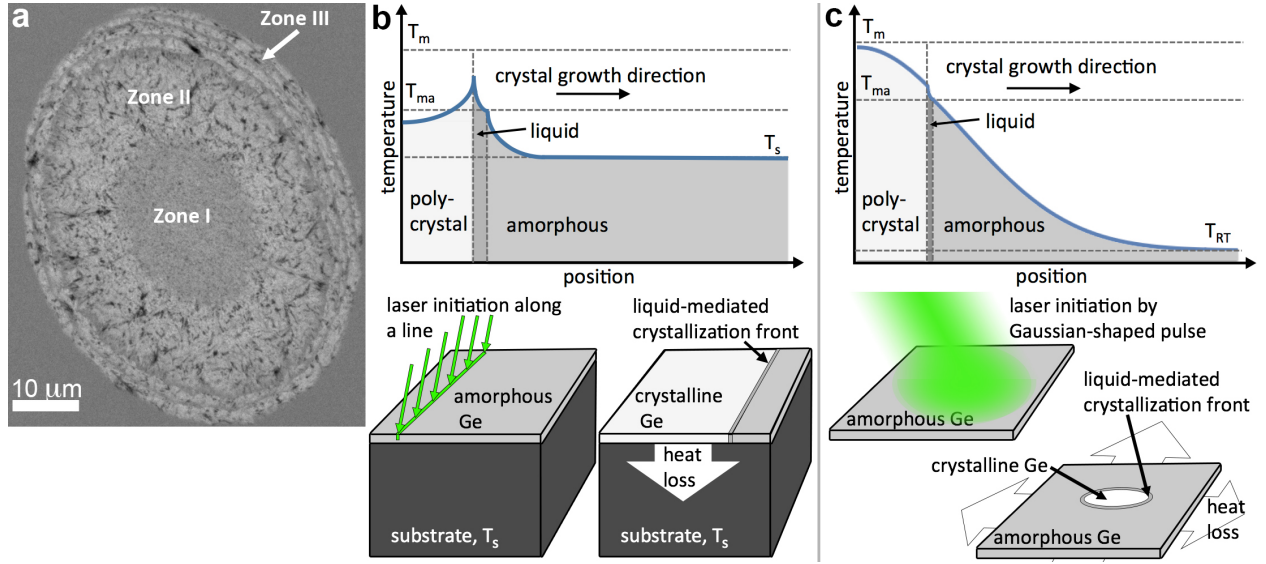
Figure 1 (Color online) (a) Conventional bright field TEM image of region crystallized by a 3.4 µJ laser shot. Zone I consists of sub-micron grains, Zone II of long radially-oriented grains, and Zone III of long grains oriented tangentially, interleaved with fine-grained material. Schematics of the experimental set-up (bottom) and temperature profile (top) during (b) liquid-mediated crystallization in a steady-state experiment where a bulk substrate is maintained at an elevated temperature, T_s, controlling the temperature and heat loss from the thin Ge film and (c) at an early stage of crystallization after a Gaussian-shaped pulse laser locally heats an electron transparent supported Ge film initially at T_{RT}. Bottom schematic of (b) adapted from ref. [13].
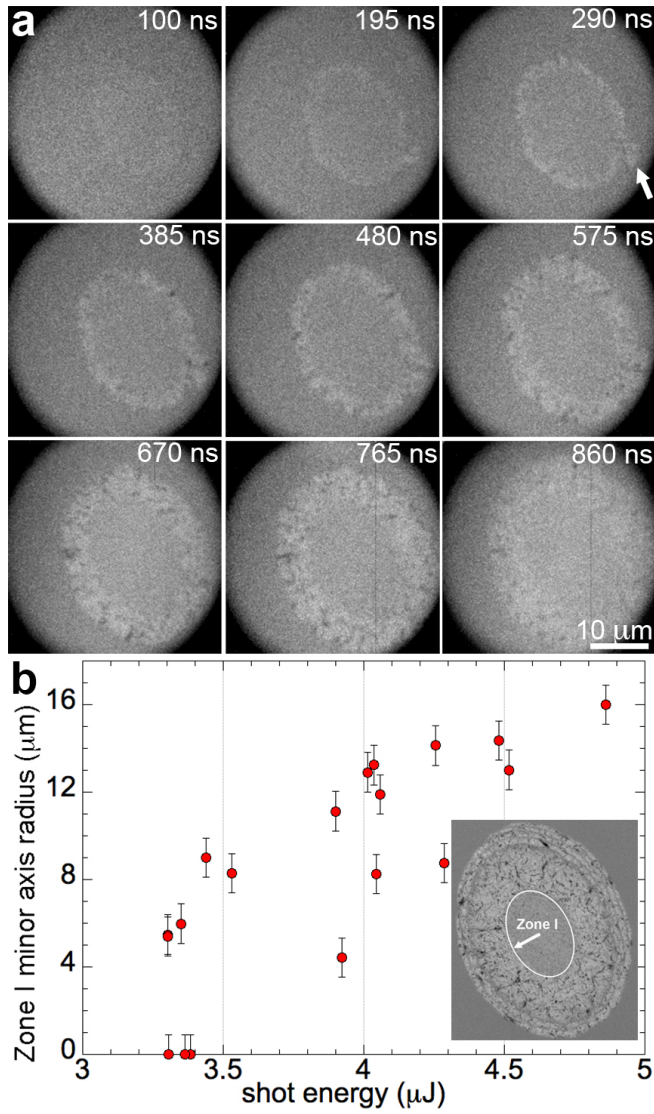
Figure 2 (a) Time-resolved images of laser-induced crystallization of the region in **Figure 1**(a), with Zone II growing out from Zone I. (b) Zone I size vs. laser energy for silica capped Ge, measured as half the minor axis of an ellipse fitted to Zone I.
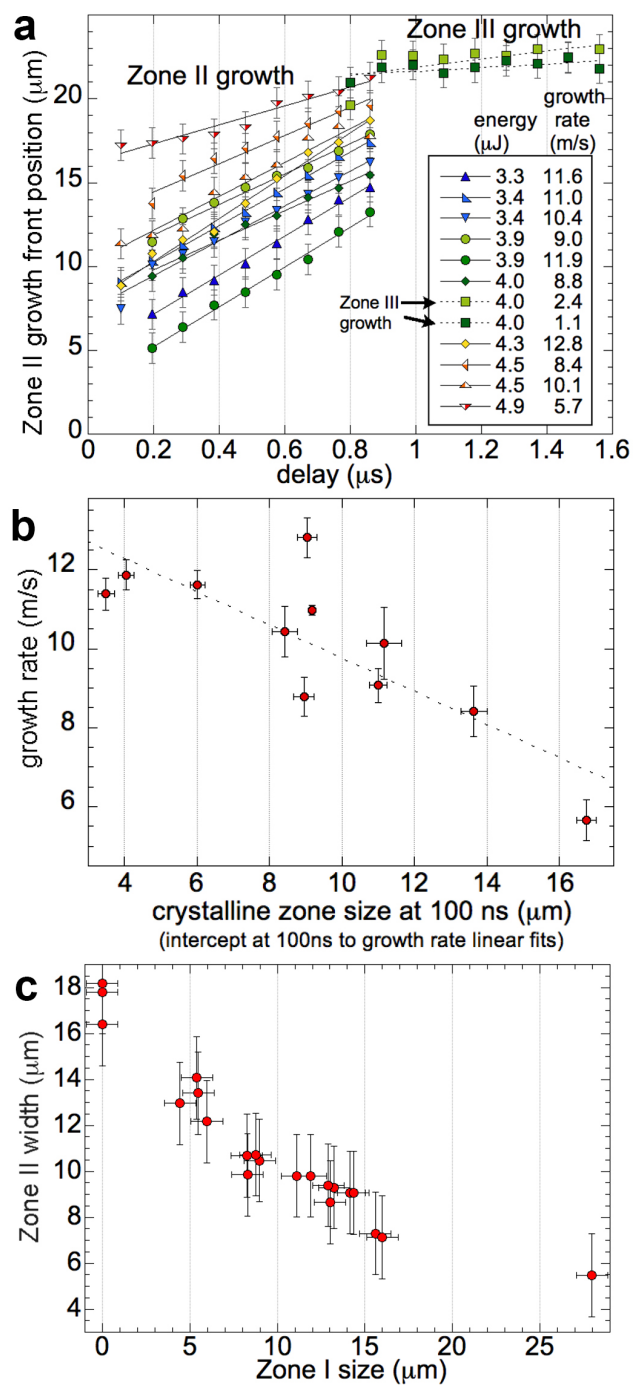
14

a

Zone II growth front position (μm)

Zone III growth

Zone II growth

energy (μJ)	growth rate (m/s)
3.3	11.6
3.4	11.0
3.4	10.4
3.9	9.0
3.9	11.9
4.0	8.8
4.0	2.4
4.0	1.1
4.3	12.8
4.5	8.4
4.5	10.1
4.9	5.7

Zone III growth

delay (μs)

b

growth rate (m/s)

crystalline zone size at 100 ns (μm)
(intercept at 100ns to growth rate linear fits)

c

Zone II width (μm)

Zone I size (μm)

Figure 3 (a) Growth front position (distance from the center to the edge of the elliptical crystalline region measured along its minor axis) as a function of time for silica-capped Ge, (b) growth rate versus zone I size, and (c) Zone II width versus Zone I size.
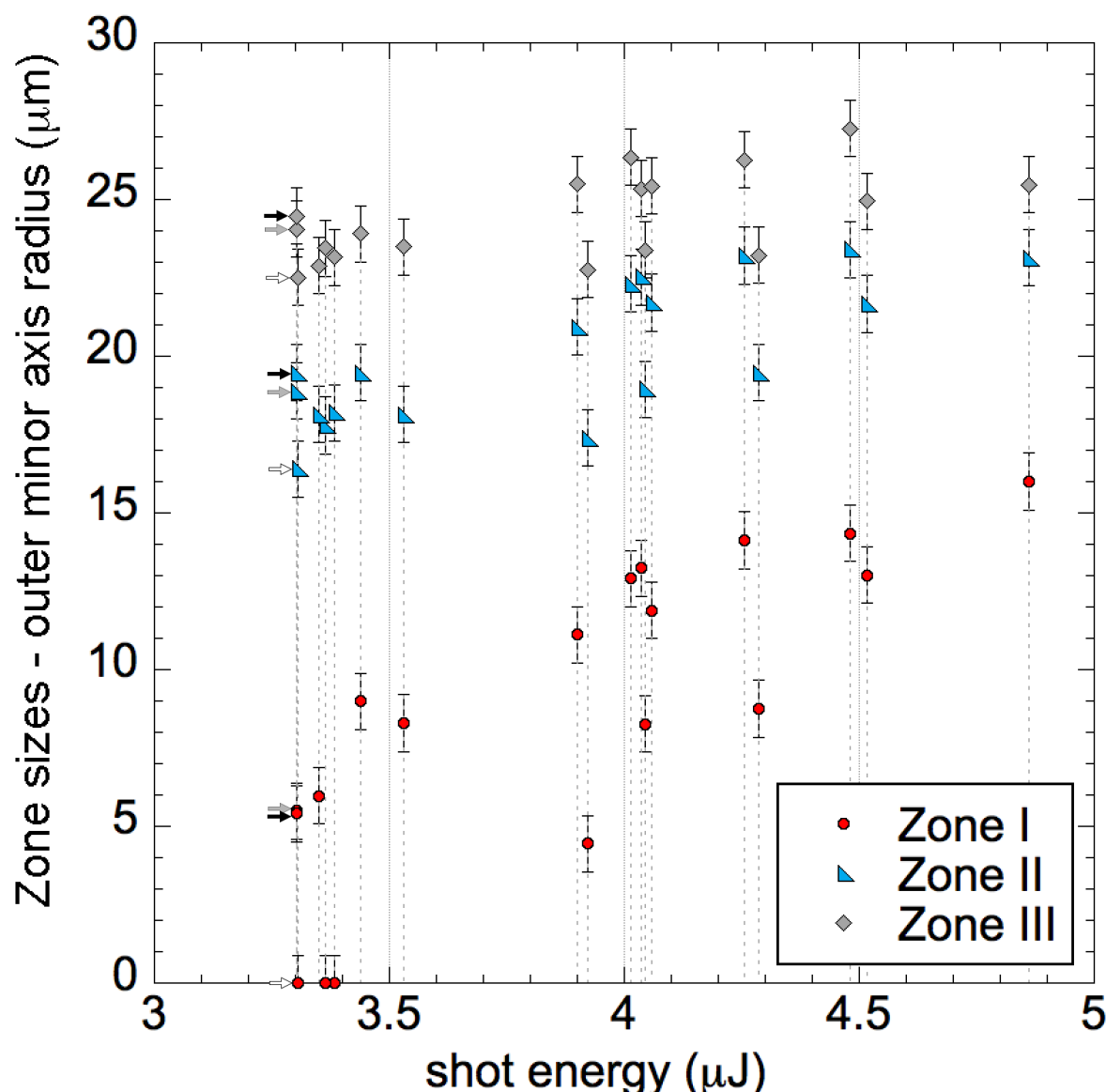
Figure S1 Zone sizes measured after laser crystallization on conventional bright-field TEM images as a function of laser pulse energy. The size of each zone is taken as the radius of the minor axis of an ellipse fitted to the outer boundary of each Zone, as illustrated for Zone I in the inset of Figure 2(a) (main text). Each set of three points connected by a drop line are zone sizes for a single spot crystallized at that energy. There are three sets of nearly overlapping measurements at 3.3 μJ. They are differentiated by set of arrows (white, gray, or black), marking each set of measurements for a single crystallization event.

The scatter in the data, gives rise to what may appear like a discontinuity in the sets of data for three 4.0 μJ shots in Figure 3a. In Figure 3(a), a 4.0 shot with measurements from 200 – 900 ns ends at a position of <15 μm. Two other ~4.0 μJ shots with measurements starting at 800 ns have the growth front >18 μm by that time. This apparent discontinuity is simply a result of the variability in crystallized area for the same (or very similar) laser energies.

There are more data points in this plot (and Figure 2(a)) than in Figure 3(a), because this figure includes measurements on conventional TEM images for which no time-resolved image was collected.
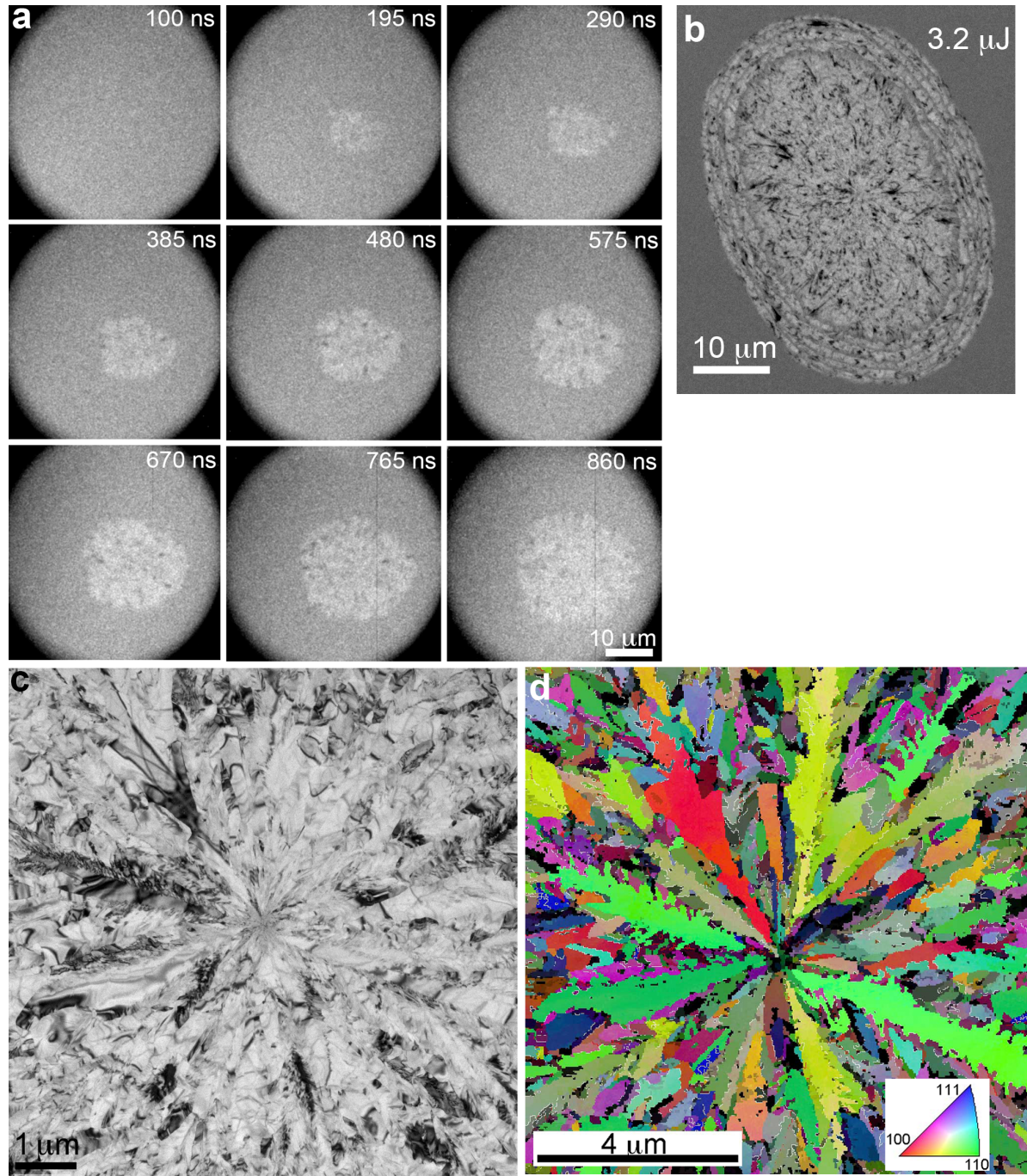
Figure S2 (a) DTEM movie of laser crystallization for the same laser pulse energy as in Figure 2a of the main text, but without the formation of Zone I. Time signatures are relative to the peak specimen laser intensity. (b) Conventional bright-field TEM image of the crystallized area in (a). It lacks the fine-grained structure of Zone I seen at the center of Figure 1a of the main text. (c) Bright-field TEM image (Philips CM300 FEG, 300kV) of the center of (b). The bend contours in the grains of the thin film make it difficult to discern individual grains, but an orientation map (d) generated from TEM nanodiffraction data makes the long narrow grains developed during Zone II growth easier to discern.
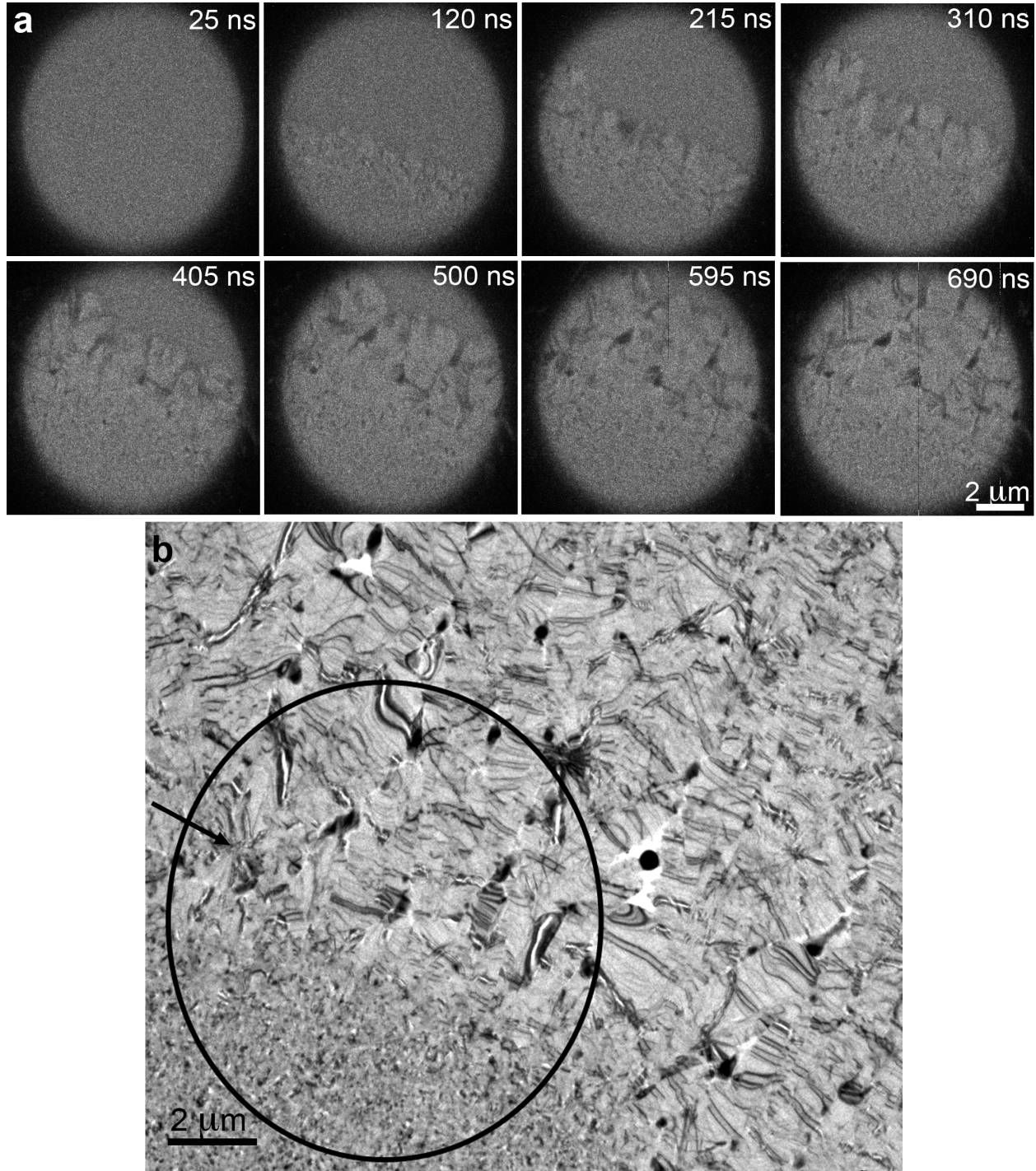
Figure S3 1200X images show unambiguously that the growth front speed is close to 10 m/s immediately after the initiation of Zone II. Zone I is formed and larger Zone II grains have begun to grow by 120 ns after the specimen is heated by the laser. Between 120 ns to 215 ns, the front moves forward by about 1 μm, except at the far left where a nucleation event makes the growth front appear to jump forward almost 2 μm. The crystal front advances by 1 μm in each subsequent frame until 595 ns, after which the front has moved out of the field of view, maintaining a fairly constant rate of just over 10 m/s for 475 ns of Zone II growth. The point where a crystalline area nucleated ahead of the rest of the front is indicted by an arrow in (b).
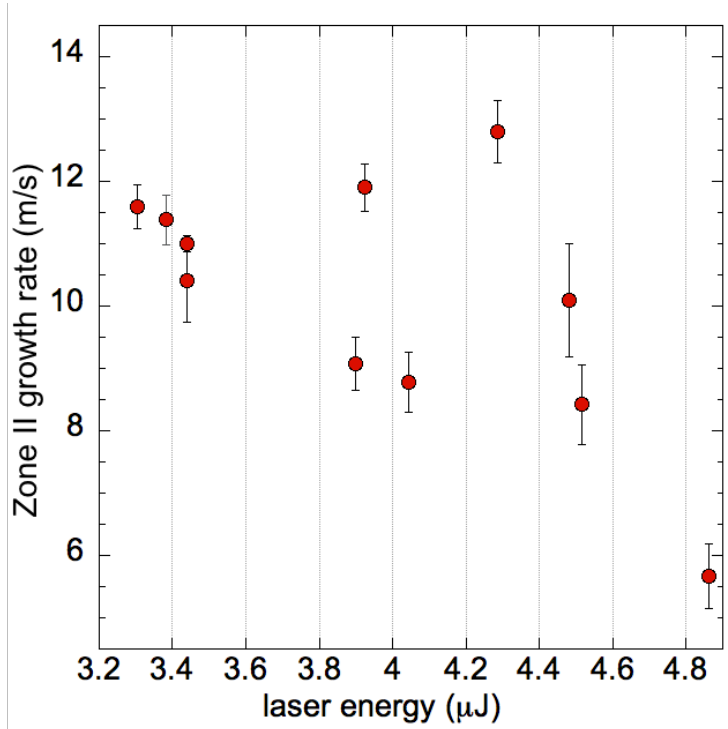
Figure S4 The Zone II growth rate plotted versus laser energy yields no strong trend in the data. The growth rate may be consolidated by plotting it against the Zone I size as shown Figure 2(b) in the main text.